Post-quench dynamics and suppression of thermalization in an open half-filled Hubbard layer

Igor V. Blinov,[1,2,*] Pedro Ribeiro,[2,3] and A. N. Rubtsov[2,4]

[1]*Moscow Institute of Physics and Technology, 9 Institutskiy Lane, Dolgoprudny, Moscow Region 141700, Russia*

[2]*Russian Quantum Center, 143025 Skolkovo, Russia*

[3]*CeFEMA, Instituto Superior Técnico, Universidade de Lisboa Avenida Rovisco Pais, 1049-001 Lisboa, Portugal*

[4]*Department of Physics, M.V. Lomonosov Moscow State University, 119991 Moscow, Russia*

(Received 26 September 2016; revised manuscript received 5 December 2016; published 20 January 2017)

We study the time evolution of a half-filled Hubbard layer coupled to a magnon bath after a quench of the Hubbard interaction. Qualitatively different regimes, regarding the asymptotic long-time dynamics, are identified and characterized within the mean-field approximation. In the absence of the bath, the dynamics of the closed system is similar to that of a quenched BCS condensate. Though the presence of the bath introduces an additional relaxation mechanism, our numerical results and analytical arguments show that equilibration with the bath is not necessarily attained within the approximations used. Instead, nonequilibrium states, similar to the ones observed in the closed system, can emerge at long times as a consequence of the competition between the intrinsic relaxation mechanism (Landau damping, for example), and the bath-induced dissipation.

DOI: 10.1103/PhysRevB.95.024309

I. INTRODUCTION

Most thermodynamic systems, if taken away from equilibrium, evolve back to an equilibrium state. The initial stage of the equilibration process often includes energy transfer from macroscopic collective excitations to the individual, microscopic degrees of freedom. The overall equilibration dynamics is thus governed by the coupling between the collective and individual modes.

Modern quantum technologies aim to store information via controlled excitation of collective states in engineered solid structures, such as various types of superconducting qubits. In order to improve quantum coherence, significant attention, both at experimental and theoretical levels, has been paid to the optimization of the decoupling between collective modes and the rest of the degrees of freedom. In certain cases, undamped collective excitations completely decoupled from the microscopic degrees of freedom were predicted theoretically. Such decoupling arises due to the existence of conservation laws present in some particular system [1]. Although the optimal degree of decoupling is model specific and the excitation lifetime is, in practice, always finite, one expects those systems to show considerable improvements in experimentally observed decoherence times.

The energy transfer from the collective to individual degrees of freedom can, in many cases, be studied using the concept of Landau damping, which does not require a detailed knowledge of the decoherence process. Landau damping appears in collisionless models and its only precondition is the causality principle. First formulated for Langmuir waves in a collisionless electron plasma [2], Landau damping is nowadays known to be a generic feature of the mean-field perturbative description of collective excitation. In particular, it appears in the BCS description of superconductors [3,4]. In this case, the collective mode is associated with deformations of the superconducting order parameter Δ and the individual degrees of freedom are Cooper pairs.

Sufficiently far away from equilibrium, regimes beyond the Landau-damping scenario may arise, such as the ones found in recent studies [5,6] of the BCS model. Here, a perturbation of the initial ground state is realized as an abrupt change (quench) of the BCS coupling parameter g from its initial value g_i to a final one g_f. For a small perturbation $g_i \approx g_f$, the dynamics can be well described by a Landau-damping scenario [4]. For $g_i \ll g_f$, as in the case of the quench from normal metal to BCS [7], a synchronization between Cooper pairs through the collective mode yields to persistent oscillations of the order parameter (phase-locked regime).

In the opposite case, $g_i \gg g_f$, the gap vanishes exponentially fast [5] (overdamped regime) since the system is effectively heated above the superconducting transition temperature.

The interplay between microscopic and collective modes has been studied in other setups [8–14], including the nonequilibrium dynamics of the half-filled Hubbard model supporting antiferromagnetic collective modes. Within the Gutzwiller approach, the after-quench dynamics of this model was shown [15] to be similar to that of the BCS model featuring all three regimes. However, because of electron-electron collisions, oscillations were found to be weakly damped in the phase-locked regime. The transition between the antiferromagnetic and paramagnetic states was also explored [16] within dynamical mean-field theory (DMFT).

The examples given below refer to closed systems. Under which conditions the asymptotic long-time state equilibrates has recently been an active topic of research [17–19]. Clearly, some of the above regimes cannot be considered as equilibrium states. Nonetheless, if equilibrium is attained, the extensive injection of energy implies that properties of the effective equilibrium state correspond to those of a finite-temperature Gibbs-like ensemble [20,21].

The presence of a weakly coupled zero-temperature reservoir is expected to radically change the physical picture [22,23]: if energy is dissipated to the bath, the system's degrees of freedom should acquire properties of the post-quench zero-temperature state. However, a competition between the system's own dissipative processes and those of the bath may

*blinov@phystech.edu

allow for other scenarios. Understanding the robustness of different dynamical regimes to the presence of an environment is a natural question as in realistic experimental situations some degree of environmental coupling is expected. The competition between dissipative effects induced by the microscopic degrees of freedom of the system or of the bath can help to shed light on the collective mode dynamics observed in recent pump-probe-like experiments.

In this work, we study the fate of nonequilibrium regimes, found in the post-quench dynamics of closed system, in the presence of a bath. In particular, we consider interaction quenches in the half-filled Hubbard model on a two-dimensional (2D) square lattice, coupled at each site to a magnetic ohmic bath. The bath degrees of freedom consist of a collection of vector bosons that couple isotropically to the local magnetization and are taken to be independent on each lattice site. The system models an antiferromagnetically ordered 2D layer in the presence of a magnon environment. Such spatially independent environment models a superparamagnetic bath medium present, for example, in disordered nanomagnets. In addition, though for a homogeneous ordered substrate spatial correlations of the bath modes may become important, our results are still relevant if the order of low-lying bath modes is incommensurate with that of the Hubbard layer. In this case, although the spatially coherent states still couple to the magnetic modes of the Hubbard layer, their ordering is not transferred to the layer.

The paper is organized as follows: Sec. II introduces the model, Sec. III describes the dynamics in the absence of any environmental coupling and identifies the different dynamical regimes in correspondence with the one in the BCS model, and Sec. IV presents the bulk of our work identifying the different dynamic regimes in the presence of the bath. A discussion and conclusions are given in Sec. V. The Appendix is devoted to study the specificities of the overdamped regime in the 2D square lattice.

II. MODEL

To study the post-quench dynamics, we consider a joint Hamiltonian of the antiferromagnetically ordered layer coupled to a magnon bath given by

$$H = H_{\text{Hub}} + H_{\text{Bath}} + H_{\text{C}}, \tag{1}$$

where

$$H_{\text{Hub}} = J \sum_{\langle \boldsymbol{r},\boldsymbol{r}'\rangle} c^{\dagger}_{\sigma \boldsymbol{r}} c_{\sigma \boldsymbol{r}} + U \sum_{\boldsymbol{r}} c^{\dagger}_{\uparrow,\boldsymbol{r}} c_{\uparrow \boldsymbol{r}} c^{\dagger}_{\downarrow \boldsymbol{r}} c_{\downarrow \boldsymbol{r}} \tag{2}$$

is the two-dimensional Hubbard Hamiltonian describing the electronic system. $c^{\dagger}_{\sigma \boldsymbol{r}}$ and $c_{\sigma \boldsymbol{r}}$ are, respectively, the fermion creation and annihilation operators of an electron on site $\boldsymbol{r}$ with spin σ. The coupling to the bosonic bath is given by

$$H_{\text{C}} = g \sum_{\boldsymbol{r}} \boldsymbol{S}_{\boldsymbol{r}} \cdot \left[\int_q (\boldsymbol{b}^{\dagger}_{q\boldsymbol{r}} + \boldsymbol{b}_{q\boldsymbol{r}}) \right], \tag{3}$$

where $S^i_{\boldsymbol{r}} = \frac{1}{2} c^{\dagger}_{\alpha \boldsymbol{r}} \tau^i_{\alpha\beta} c_{\beta \boldsymbol{r}}$ is the spin operator of the electrons at the $\boldsymbol{r}$th site and $\tau^{i=x,y,z}_{\alpha\beta}$ denote the Pauli matrices. $b^{i\dagger}_{q\boldsymbol{r}}$, $b^i_{q\boldsymbol{r}}$ are creation and annihilation operators of the vector bosons. The magnon environment is assumed to be spatially incoherent; therefore the summation over bosonic momentum index q is performed independently for each site index $\boldsymbol{r}$. The Hamiltonian of the bath is

$$H_{\text{Bath}} = \sum_{\boldsymbol{r}} \int_q \Omega_q \boldsymbol{b}^{\dagger}_{q\boldsymbol{r}} \cdot \boldsymbol{b}_{q\boldsymbol{r}}. \tag{4}$$

The two-dimensional antiferromagnet magnon bath has an ohmic density of states of the form $\rho(\epsilon) = \int_q \delta(\epsilon - \Omega_q) = \frac{\epsilon}{C^2} e^{-\frac{\epsilon}{\Lambda}}$, where Λ is a high-energy cutoff and C is a constant with dimension of energy. In the following, we set $C = 1$ and measure all other energies in units of C. In all numerical results, we set $\Lambda = 20$, $J = 2$. No qualitative changes arise by changing the cutoff Λ as long as it is taken to be much larger than all other energies scales.

We study the dynamics of the magnetization after an interaction quench where the value of U is switched from $U = U_i$ to $U = U_f$ at $t = 0$. We treat the system within a mean-field approximation assuming the spin fluctuations are small compared with the average magnetization. For all of the analyzed cases, the initial state is the ground state of the system for $U = U_i$ obtained within the mean-field approach.

III. CLOSED SYSTEM

In this section, we study quenches of the closed system, i.e., when the coupling to the bath, g, is set to zero. First, we derive the set of mean-field equations governing the post-quench dynamics. We then analyze the long-time asymptotic dynamics, establishing the parallels and differences to previous studies of the BCS model.

For the isolated electronic system described by Eq. (2), the mean-field approximation is valid for time scales less than $\tau_q \sim E_F/\Delta^2$, after which interactions between quasiparticles can no longer be neglected [7]. The mean-field Hamiltonian can be obtained from Eq. (2) by neglecting second-order magnetic fluctuation terms $(\boldsymbol{S}_{\boldsymbol{r}} - \langle \boldsymbol{S}_{\boldsymbol{r}} \rangle)^2$ and assuming a spin ordered state $\langle \boldsymbol{S}_{\boldsymbol{r}} \rangle = \boldsymbol{M} \cos(\boldsymbol{Q} \cdot \boldsymbol{r})$ with ordering wave vector $\boldsymbol{Q}$ [24].

A systematic approach for the construction of a mean-field approximation can be obtained within the functional integral formalism and amounts to a decoupling of fermionic fields using the Hubbard-Stratonovich transformation [25]. The latter step, while mathematically exact, induces an ambiguity (sometimes alluded to as Fierz ambiguity [26]) related to the choice of the decoupling channel that conditions further approximations. In this work, we deal exclusively with a half-filled Hubbard layer known to have a magnetic instability towards the formation of an antiferromagnetic state. Therefore, on physical grounds, we have chosen a decoupling in the magnetic exchange channel as this gives the leading contribution to free energy. We thus consider an antiferromagnetic state, i.e., $\boldsymbol{Q} = \{\pi, \pi\}$, magnetized along the z axes, $\boldsymbol{M} = M \boldsymbol{e}_z$, corresponding to a mean-field Hamiltonian of the form

$$H_{\text{MF}} = \int_k \epsilon_{\boldsymbol{k}} c^{\dagger}_{\sigma \boldsymbol{k}} c_{\sigma \boldsymbol{k}} + \frac{2U}{3} M^2 - \frac{4U}{3} S^z_{\boldsymbol{Q}} M, \tag{5}$$

with $\boldsymbol{k}$ labeling the two-dimensional momentum and $\int_k = \int \frac{d^2k}{(2\pi)^2}$ the Brillouin-zone integration. $\epsilon_{\boldsymbol{k}} = 2J(\cos k_x + \cos k_y)$ is the dispersion relation and $S^z_{\boldsymbol{Q}} = \frac{1}{2} \int_k c^{\dagger}_{\sigma \boldsymbol{k}} \tau^z_{\sigma\sigma'} c_{\sigma' \boldsymbol{k}+\boldsymbol{Q}}$ is the staggered spin operator in the z direction.

The dynamics can most easily be described in terms of pseudospins, which are similar to Anderson representation [27]:

$$\hat{\tau}^x_{\sigma\boldsymbol{k}} = \tfrac{1}{2}(c^\dagger_{\sigma\boldsymbol{k}} c_{\sigma\boldsymbol{k}+\boldsymbol{Q}} + c^\dagger_{\sigma\boldsymbol{k}+\boldsymbol{Q}} c_{\sigma\boldsymbol{k}}), \tag{6}$$

$$\hat{\tau}^y_{\sigma\boldsymbol{k}} = \tfrac{i}{2}(c^\dagger_{\sigma\boldsymbol{k}} c_{\sigma\boldsymbol{k}+\boldsymbol{Q}} - c^\dagger_{\sigma\boldsymbol{k}+\boldsymbol{Q}} c_{\sigma\boldsymbol{k}}), \tag{7}$$

$$\hat{\tau}^z_{\sigma\boldsymbol{k}} = \tfrac{1}{2}(c^\dagger_{\sigma\boldsymbol{k}} c_{\sigma\boldsymbol{k}} - c^\dagger_{\sigma\boldsymbol{k}+\boldsymbol{Q}} c_{\sigma\boldsymbol{k}+\boldsymbol{Q}}), \tag{8}$$

defined for each spin projection σ. Assuming that the initial state respects the symmetries of H_{MF}, the expectation values for the two spin projections are simply related by

$$\langle \hat{\tau}^x_{\uparrow\boldsymbol{k}} \rangle = -\langle \hat{\tau}^x_{\downarrow\boldsymbol{k}} \rangle, \tag{9}$$

$$\langle \hat{\tau}^y_{\uparrow\boldsymbol{k}} \rangle = -\langle \hat{\tau}^y_{\downarrow\boldsymbol{k}} \rangle, \tag{10}$$

$$\langle \hat{\tau}^z_{\uparrow\boldsymbol{k}} \rangle = \langle \hat{\tau}^z_{\downarrow\boldsymbol{k}} \rangle. \tag{11}$$

Therefore, in the following, we set $\hat{\tau}^\alpha_{\boldsymbol{k}} = \hat{\tau}^\alpha_{\uparrow\boldsymbol{k}}$ in order to simplify the notation. In terms of the pseudospin variables τ, the equations of motion can be written in a closed form,

$$\frac{d}{dt}\langle \hat{\boldsymbol{\tau}}_{\boldsymbol{k}}(t) \rangle = 2\boldsymbol{B}_{\boldsymbol{k}}(t) \times \langle \hat{\boldsymbol{\tau}}_{\boldsymbol{k}}(t) \rangle, \tag{12}$$

where $\boldsymbol{B}_{\boldsymbol{k}}(t) = \{h_c(t), 0, \epsilon_{\boldsymbol{k}}\}$, with $h_c(t) = -4U(t)M(t)/3$ and the self-consistent condition

$$M(t) = \int_k \langle \hat{\tau}^x_{\boldsymbol{k}}(t) \rangle. \tag{13}$$

For the quench protocol studied here, $U(t > 0) = U_f$. The initial conditions, obtained by starting from the ground state of H_{MF} with $U(t = 0) = U_i$, are given by

$$\langle \hat{\boldsymbol{\tau}}_{\boldsymbol{k}}(t = 0) \rangle = -\frac{\boldsymbol{B}_{\boldsymbol{k}}(t = 0)}{2\sqrt{\epsilon^2_{\boldsymbol{k}} + h_c(t = 0)^2}}. \tag{14}$$

This result can be derived by minimizing the mean-field energy, which in terms of the pseudospin τ is given by $E_{\mathrm{MF}} = \langle H_{\mathrm{MF}} \rangle = 2\int_k \boldsymbol{B}_{\boldsymbol{k}} \cdot \langle \hat{\boldsymbol{\tau}}_{\boldsymbol{k}} \rangle$ with respect to the order parameter $M(t = 0)$.

The mean-field dynamics obtained by this procedure is closely related to that of the BCS model [5,15,16]. In fact, the equations of motion (12) and those of the BCS Hamiltonian can be mapped to each other by a suitable identification of physical quantities. The main difference between the two models comes from the dispersion relation $\epsilon_{\boldsymbol{k}}$ that in the BCS model is usually taken to be that of a free-electron gas, yielding in 2D to a constant density of states within the Debye window. Here, the fact that $\epsilon_{\boldsymbol{k}}$ admits the nesting wave vector $\boldsymbol{Q}$ at half filling is crucial for the establishment of the antiferromagnetic instability and therefore has to be explicitly taken into account.

In the reminder of this section, we study the different dynamical regimes of the asymptotically large time dynamics of the post-quench evolution governed by Eq. (12). The different regimes are similar to those of the BCS model [16], but crucial differences arise nonetheless in the approach to the long-time limit due to the particular features of the dispersion relation.

The upper panel of Fig. 1 shows the phase diagram in the $U_f - U_i$ parameter space. As in the BCS case, there are three different regimes, shown in the lower panels of Fig. 1:

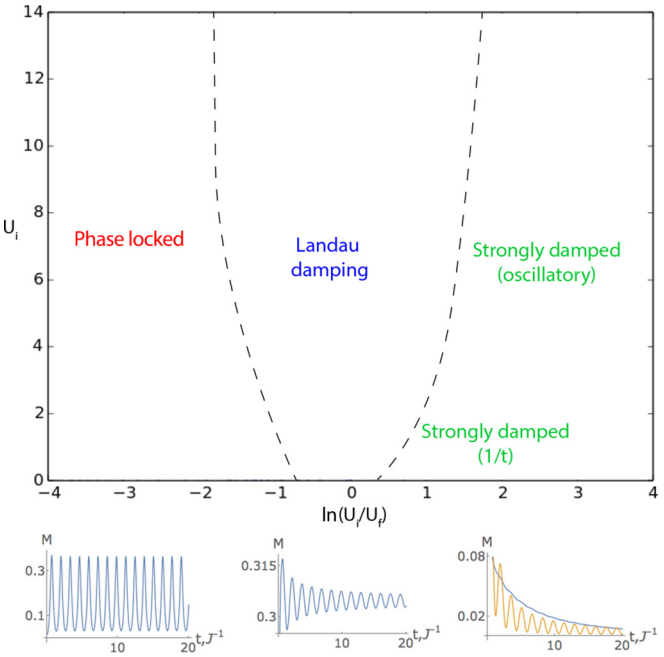

FIG. 1. Upper panel: Sketch of the phase diagram as a function of U_f and U_i. Lower panels (left to right): Examples of the different dynamical regimes, i.e., phase locked, $U_i = 0.8$, $U_f = 12$; Landau damping, $U_i = 4$, $U_f = 5$; and overdamped, $U_i = 3$, $U_f = 0.5$.

(i) The phase-locked regime, arising for $U_i/U_f \ll 1$, is characterized by nonvanishing oscillations of the order parameter. This behavior is similar to the one described in [7]: the collective mode synchronizes the different momentum pseudospin precessions.

(ii) The Landau-damping regime, for $U_i/U_f \approx 1$, where the order parameter attains a nonvanishing constant value. Here, oscillations decay as $\propto \frac{1}{\sqrt{t}}$ as in the BCS case [28]. The mechanism behind this kind of damping is similar to the one first found in plasma [2]: as in the BCS case [3,5], a collective mode interacts with quasiparticles with energies around 2Δ, where Δ is an antiferromagnetic gap.

(iii) The overdamped regime, when $U_i/U_f \gg 1$, where the order parameter vanishes at large times. As in the BCS case [28], the order parameter drops to zero. However, instead of the exponential decay observed for BCS, the decay is algebraic in $1/t$ and a crossover is observed as a function of U_i from damped-oscillatory to purely damped behavior in the dynamics of $M(t)$. This behavior, overlooked in similar setups [15,16], is due to the nonanalyticities of the density of states in two dimensions: a logarithmic divergence near the Fermi surface and a sharp cutoff at the band edges. A detailed analysis of the crossover is given in the Appendix.

IV. OPEN SYSTEM

We now address the changes in the dynamics of the system in the presence of the environment. In the following, we generalize the equations of motion to account for the magnetic bath and analyze the different dynamical regimes.

Following the same steps as before, the mean-field Hamiltonian is given by

$$H_{\mathrm{MF}} = \int_k \epsilon_{\boldsymbol{k}} c^\dagger_{\sigma \boldsymbol{k}} c_{\sigma \boldsymbol{k}} + \frac{2U}{3} M^2 - \frac{4U}{3} S^z_{\boldsymbol{Q}} M + g M \int_q \left(b^{z\dagger}_q + b^z_q \right) + \int_q \Omega_q b^{z\dagger}_q b^z_q. \quad (15)$$

In addition to the pseudospin degrees of freedom, the dynamics of the bosonic fields has to be considered. At the mean-field level, this can be done by explicitly solving the equation of motion for the bosonic fields, $\frac{d}{dt} b^z_q = i[H_{\mathrm{MF}}, b^z_q]$. Similarly to the case of the closed system, the initial state is taken to be the ground state of the whole system. Substituting in the equations of motion of pseudospins, we get a closed system of equations that has the same form (12) as in the isolated case, but with a different "pseudo magnetic field" $\boldsymbol{B_k}(t) = \{h_d(t), 0, \epsilon_k\}$ where

$$h_d(t) = -\frac{2U(t)M(t)}{3} - g^2 \frac{\Lambda M(0)}{1+\Lambda^2 t^2} - 2g^2 \int_0^t d\tau \frac{\Lambda^3 M(\tau)(t-\tau)}{[1+\Lambda^2(t-\tau)^2]^2}. \quad (16)$$

As before, $M(t)$ respects the self-consistency condition (13) and $M(0)$ is the initial value of the staggered magnetization.

Before studying the effects of the environment in different dynamic regimes, let us analyze the stationary solutions $M(t) \equiv M$ in the presence of the environment. In this case, h_d simplifies to

$$h_d = -2\left(\frac{2U}{3} + g^2 \Lambda \right) M. \quad (17)$$

This stationary condition is equivalent to that of the closed system with a renormalization of the value of the coupling $U \to U_{\mathrm{R}} = U + \frac{3g^2\Lambda}{2}$. Therefore, the only effect of environment on the equilibrium properties of the electronic subsystem is a renormalization of the coupling constant. Since the renormalization of U is always positive, the presence of the environment always enhances the antiferromagnetic order.

It is worth noting that in case the system approaches such stationary solution (not necessary an equilibrium one), the equations of motion of the open system reduce to those of the closed one with a renormalized U. This can be most easily shown by introducing a time scale T_{stat} after which $M(t)$ is close to the stationary value M_{stat}. For times $1/\Lambda \ll T_{\mathrm{stat}} \ll t$, up to terms of order t/T_{stat} and $1/(\Lambda t)^2$, one has

$$h_d(t) \approx h_{\mathrm{stat}} - \frac{2g^2\Lambda[M(0) - M_{\mathrm{stat}}]}{(\Lambda t)^2} - \frac{4g^2}{(\Lambda t)^3} \int_0^{T_{\mathrm{stat}}} d\tau M(\tau), \quad (18)$$

which when $t \to \infty$ tends to $h_{\mathrm{stat}} = -\frac{4U_f M_{\mathrm{stat}}}{3} - 2g^2 \Lambda M_{\mathrm{stat}}$. Thus, for sufficiently large times, in the approach to M_{stat} the individual degrees of freedom τ^x_k are governed by the renormalized electronic dynamics. Consequently, we may conclude that whenever configuration with stationary M_{stat} (not necessarily equilibrium) has been reached, the environment's role is reduced to renormalization of U. This argument is essential for understanding the absence of thermalization in overdamped and damped regimes, which will be described below.

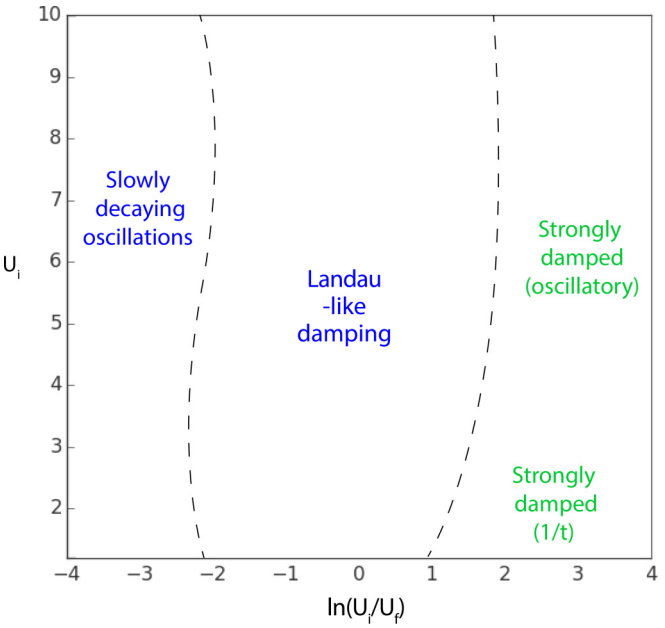

FIG. 2. Sketch of the phase diagram for an open system for $g = 0.25$. With increasing of g, the damped regime expands, pushing its boundaries in both directions. This arises due to the renormalization of U (see text) that decreases the effective amplitude of the quench.

In the following, it is important to distinguish between two kinds of stationary solution: equilibrium states where M_{stat} minimizes the mean-field energy and yields no dynamics to the pseudospins $d\langle \hat{\boldsymbol{\tau}}_{\boldsymbol{k}} \rangle / dt = 0$, and nonequilibrium states where $d\langle \hat{\boldsymbol{\tau}}_{\boldsymbol{k}} \rangle / dt \neq 0$. In the case of a closed system, conservation of energy implies that only nonequilibrium stationary states can be attained as is the case of the final state of the Landau damped regime. In the presence of a bath, even if the total energy is still conserved, a change of energy of the system can be absorbed by the bath with no macroscopic changes in any intensive bath observable. It is naively expectable that by absorbing the excess energy, the environment renders the system observables to their equilibrium values. Nonetheless, as shown below, both equilibrium and nonequilibrium solutions may arise for the open system.

Figure 2 shows a sketch of the phase diagram of the open system for different values of the coupling g. Approximate boundaries between phases were estimated using $N = 150$. In particular, the boundary between the regime with slowly decaying oscillations and the Landau-like damped case was estimated by plotting the order parameter $\Delta M(T_N) = [M(T_N) - M_{\mathrm{eq}}]/M_{\mathrm{eq}}$, where $T_N \propto N$ is the largest time for which the evolution does not depict any finite-size effects (see Sec. IV and Fig. 5 for details). With the present numerical data, one cannot determine boundaries precisely; therefore the sketch in Fig. 2 provides only a qualitative understanding of their mutual arrangement. The nonmonotonic behavior of the left boundary can be an artifact of the method. The three phases found are reminiscent of those described for the closed system. In the following sections, we present our numerical results obtained by solving the equations of motion and give

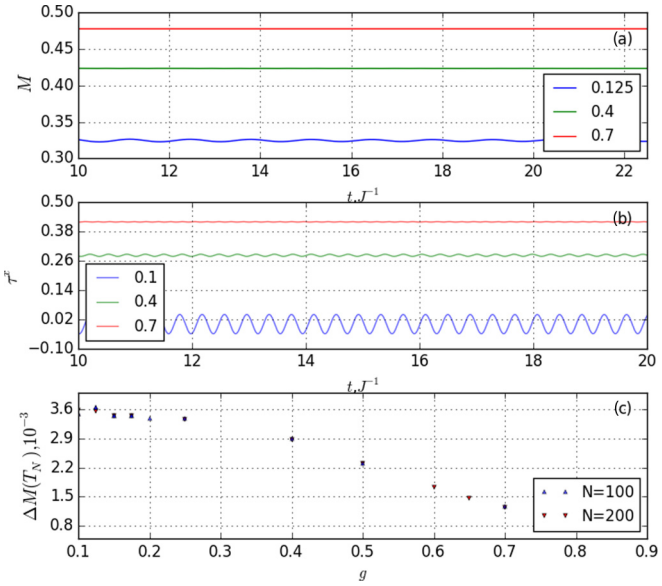

FIG. 3. Impact of the bath on the post-quench dynamics. Damped regime described in Sec. IV A, for $U_i = 4.5$ to $U_f = 5$, $\Lambda = 20$. (a) Time evolution of staggered magnetization for several values of g and $N = 200$. (b) Time evolution of individual mode τ^x_k for several values of g and $N = 200$ computed for a generic value of the momentum $k = \{2\pi/(N-1), \pi/(N-1)\}$. (c) Dimensionless parameter $\Delta M(T_N)$ as a function of g for two values of N. The finite-size times were taken to be $T_{N=100} = 23$, $T_{N=200} = 45$.

analytical arguments in order to characterise the nature of each phase.

The equation of motion (12), with the memory kernel defined in Eq. (16), was solved numerically using a fourth-order Runge-Kutta method. The integral in Eq. (16) was calculated at each step by employing Simpson's rule. Calculations were performed on a discrete momentum grid corresponding to a finite system with periodic boundary conditions and linear size N. Accordingly, k-space integrals were substituted by discrete sums: $\int_k \to \frac{1}{N^2}\sum_k$. All of the numerics were done using $J = 2$.

A. Damped regime

As argued before, in the mean-field description of the open system, the presence of the dissipative bath only seems to qualitatively affect the evolution as long as $M(t)$ is time dependent; for $M(t) = M$, its effect simply amounts to a renormalization of the interaction constant. This helps to understand $U_f \simeq U_i$ quenches, corresponding to the Landau-damping regime in the closed system. Figure 3(a) shows the time evolution of the order parameter for different values of the environment coupling g. As in the closed case, one observes a decay of the persistent oscillations and the establishment of an asymptotic stationary state that differs from the equilibrium one. Figure 5(b) further corroborates that $M_{\rm stat} \neq M_{\rm eq}$ as the dynamics of the pseudospins seems to be nontrivial, $d\langle\hat{\boldsymbol{\tau}}_{\boldsymbol{k}}\rangle/dt \neq 0$, in the long-time limit.

Figure 3(c) shows the rescaled deviation from equilibrium of the order parameter $\Delta M(T_N) = [M(T_N) - M_{\rm eq}]/M_{\rm eq}$ as a function of g for different system sizes. $T_N \propto N$ is the largest time for which the evolution does not depict any finite-size effects. Defined in this way, $\Delta M_\infty = \lim_{N\to\infty} \Delta M(T_N)$ vanishes in the equilibrated phase and is nonzero for nonequilibrium stationary solutions. We observe that $\Delta M(T_N)$ appears to be converged to ΔM_∞ for the considered sizes. The decreasing of ΔM_∞ with the coupling to the bath is due to the fact that for larger g, both the initial and the final values of the renormalized U increase with g^2; therefore, the relative quench magnitude decreases and thus, in the large-g limit, the quenched system is asymptotically close to the equilibrium one.

In order to understand this behavior, we proceed as in the closed case and consider the quench to be a small perturbation $\delta M/M(\infty) \ll 1$, with $\delta M = M(\infty) - M_{\rm eq}$, where $M_{\rm eq}$ is the equilibrium value of the magnetization at $U = U_f$. The solution of the equations of motion (12) is assumed to be of the form $\langle\hat{\boldsymbol{\tau}}_{\boldsymbol{k}}(t)\rangle = \langle\hat{\boldsymbol{\tau}}_{\boldsymbol{k}}\rangle_{\rm eq} + \boldsymbol{s}_{\boldsymbol{k}}(t)$ and $M(t) = M_{\rm eq} - \delta(t)$, where $\langle\hat{\boldsymbol{\tau}}_{\boldsymbol{k}}\rangle_{\rm eq}$ is the equilibrium value of the pseudospin for $U = U_f$. Expanding Eq. (12) to first order for $s^x_{\boldsymbol{k}}$, $\delta(t)$, and δM, one obtains

$$\frac{d}{dt}\boldsymbol{s}_{\boldsymbol{k}}(t) \approx 2\begin{pmatrix} b_x(t) \\ x0 \\ \epsilon_k \end{pmatrix} \times \boldsymbol{s}_{\boldsymbol{k}}(t), \tag{19}$$

with $b_x(t) = -\frac{4UM_{\rm eq}}{3} + 2g^2\frac{\Lambda\delta M}{1+\Lambda^2t^2} - 2g^2\Lambda M_{\rm eq}$. Further simplifying the equation by assuming $t \to \infty$, one gets, explicitly,

$$\begin{aligned} \frac{d}{dt}s^x_{\boldsymbol{k}}(t) &\approx -2\epsilon_{\boldsymbol{k}}s^y_{\boldsymbol{k}}, \\ \frac{d}{dt}s^y_{\boldsymbol{k}}(t) &\approx 2\epsilon_{\boldsymbol{k}}s^x_{\boldsymbol{k}} + 2b_x s^z_{\boldsymbol{k}}, \\ \frac{d}{dt}s^z_{\boldsymbol{k}}(t) &\approx -2b_x s^y_{\boldsymbol{k}}, \end{aligned} \tag{20}$$

with $b_x = \lim_{t\to\infty} b_x(t) = -\frac{4UM_{\rm eq}}{3} - 2g^2\Lambda M_{\rm eq}$. The solution for s^x is thus of the form

$$s^x_{\boldsymbol{k}}(t) \approx C_{\boldsymbol{k}}\frac{\epsilon_{\boldsymbol{k}}\cos\left[2\sqrt{\epsilon^2_{\boldsymbol{k}} + \left(\frac{4U_{\rm R}M_{\rm eq}}{3}\right)^2}\,t\right]}{\sqrt{\epsilon^2_{\boldsymbol{k}} + \left(\frac{4U_{\rm R}M_{\rm eq}}{3}\right)^2}}, \tag{21}$$

where the constants $C_{\boldsymbol{k}}$ are determined by the initial condition and the previous evolution of the system for times smaller than $t \simeq \Lambda^{-1}$. The form of Eq. (21) is the same as the one for the closed system [28] with U_f substituted by $U_{\rm R}$. Besides this renormalization factor, the only impact of the bath is accounted for in the coefficients $C_{\boldsymbol{k}}$. Thus, in this regime, the dynamics of the individual degrees of freedom of the open system are qualitatively similar to that of the closed one. Nonetheless, the dependence of $C_{\boldsymbol{k}}$ on the bath makes the exponent ν, governing the approach to the asymptotic value $M(t) \simeq M(\infty) + O(t^{-\nu})$, different from the Landau-damping result $\nu = 1/2$. Figure 4 shows a log-log plot of the staggered magnetization as a function of time. In order to estimate ν, we fit the local maxima to the function $-\nu_N(g)\ln(t) + a$. The exponent ν is found to have a substantial dependence on g: it varies from $\nu_{200}(g = 0.0) \approx 0.5$ to $\nu_{200}(g = 0.25) \approx 0.9$ smoothly. Finite-size effects were found to be negligible for $N = 150$ and $N = 200$.

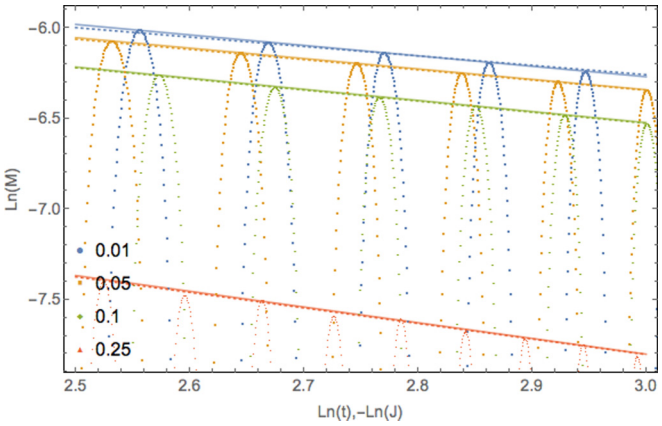

FIG. 4. Influence of bath on exponents $\nu_N(g)$ in the damped regime ($U_i = 4.5$ to $U_f = 5$, $\Lambda = 20$) for different values of coupling g and different system sizes (solid line for $N = 150$ and dotted for $N = 100$, coincide for all g's). Exponents were computed by fitting maximums of staggered magnetization to linear function $-\nu_N(g)\ln(t) + a$ (solid line).

B. Equilibrating regime

For quenches with $U_f \gg U_i$, roughly corresponding to the phase-locked regime in a closed system, the presence of the dissipative bath leads to the decay of the persistent oscillations and the establishment of an asymptotic equilibrium state. Figure 5(a) shows the evolution of the order parameter for different values of the environment coupling g. For the smaller values of g, the long time $M(t \to \infty)$ attains the equilibrium value. For the larger values of g, this is no longer the case. Figure 5(b) shows that these two asymptotic regimes correspond to the trivial $d\langle\hat{\tau}_k\rangle/dt = 0$ and nontrivial $d\langle\hat{\tau}_k\rangle/dt \neq 0$ dynamics of the pseudospins. Figure 5(c) shows the rescaled deviation from equilibrium of the order parameter $\Delta M(T_N)$ as a function of g for different system sizes. The finite-size scaling with N shows that in the equilibrated phase, $\Delta M(T_N)$ vanishes with increasing N, while for larger g, it attains a finite value. The presence of a fixed point around $g \approx 0.2$ indicates a dynamical phase transition between the two regimes.

The fact that the system does not equilibrate for large system-bath coupling seems rather counterintuitive. This can, however, be explained by the fact that besides dissipation, i.e., the appearance of a memory kernel in the evolution, the presence of the environment also renormalizes the coupling constant U and thus the system moves into a Landau-like damping regime where equilibration with the environment does not happen.

The fact that the amplitude of oscillations that were persistent in the closed system now decreases with time can be understood in the following way: without bath, a phase-locked collective mode cannot transfer energy to individual modes due to the presence of the energy gap, while in the open system, there are always bath modes to which energy may be transferred. As a result, the excited state decays. Moreover, since the energy exchange between the collective and the individual quasiparticle modes is suppressed, there is no electronic relaxation mechanism available other than the bath. Therefore, the only possibility for the system is to equilibrate with it.

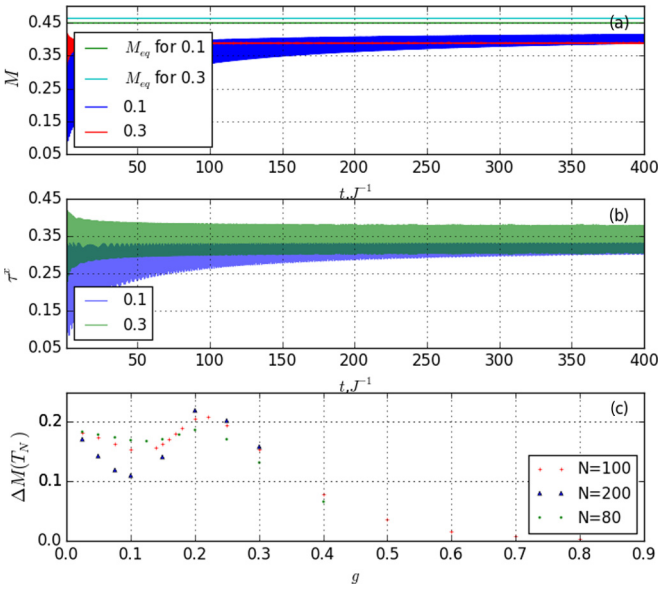

FIG. 5. Impact of the bath on the post-quench dynamics. Equilibrated and damped regimes ($U_i = 0.8$ to $U_f = 12$, $\Lambda = 20$). (a) Time evolution of staggered magnetization for several values of g and $N = 100$. (b) Time evolution of individual mode τ_k^x for several values of g and $N = 100$ computed for a generic value of the momentum $k = \{2\pi/(N-1), \pi/(N-1)\}$. (c) Dimensionless parameter $\Delta M(T_N)$ as a function of g for three values of N. The finite-size times were taken to be $T_{N=80} = 23$, $T_{N=100} = 45$, and $T_{N=200} = 250$.

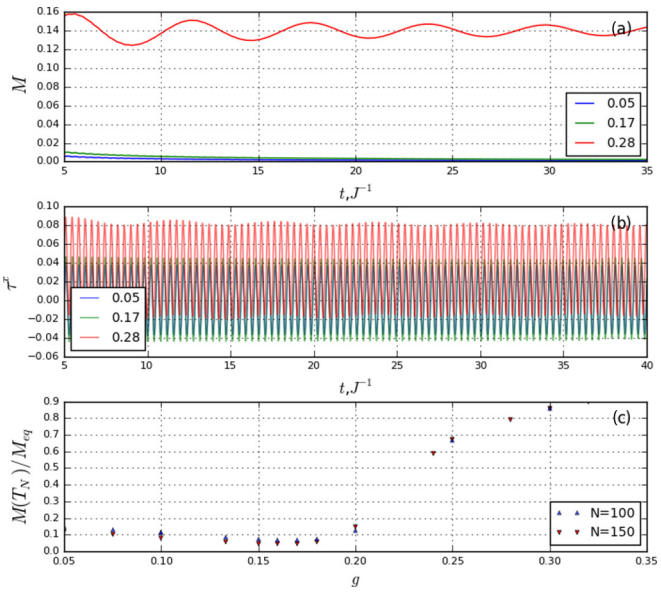

FIG. 6. Impact of the bath on the post-quench dynamics. Overdamped and damped regimes ($U_i = 3.0$ to $U_f = 0.5$, $\Lambda = 20$). (a) Time evolution of staggered magnetization for several values of g and $N = 150$. (b) Time evolution of individual mode τ_k^x for several values of g and $N = 150$ computed for a generic value of the momentum $k = \{2\pi/(N-1), \pi/(N-1)\}$. (c) Dimensionless parameter $M(T_N)/M_{\text{eq}}$ as a function of g for two values of N. The finite-size times were taken to be $T_{N=100} = 23$, $T_{N=150} = 35$.

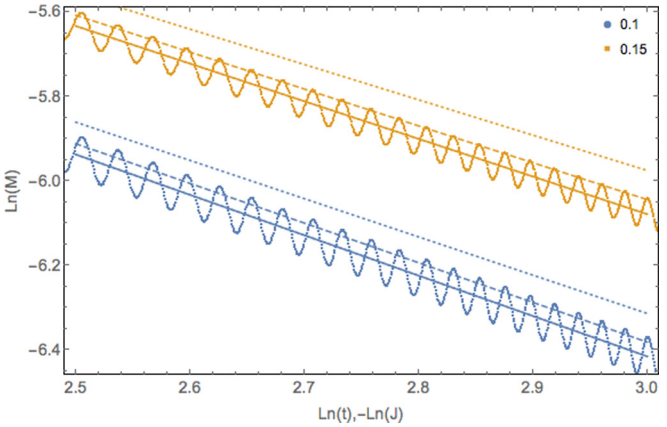

FIG. 7. Exponents $\nu(g)$ in the overdamped ($U_i = 3.0$ to $U_f = 0.5$, $\Lambda = 20$) regime for different values of coupling g and different system sizes. Exponents were computed by fitting (solid line for linear size $N = 200$, dashed line for $N = 150$, dotted line for $N = 100$) of the averages of the time dependence of the logarithm of staggered magnetization (plotted only for $N = 200$) by linear function $-\nu_N(g)\ln(t) + a$.

C. Overdamped regime

In the overdamped regime arising for $U_f \ll U_i$, the interaction with the bath does not qualitatively change the dynamics with respect to the $g = 0$ case apart from the renormalization of U. A fast decay of the order parameter to $M(\infty) = 0$ can be observed for the small values of g depicted in Fig. 6(a). For larger values of g, the damped regime sets in and $M(\infty)$ is nonvanishing. Figure 6(b) shows that even if $M(\infty) = 0$, the microscopic dynamics $\langle \hat{\boldsymbol{\tau}}_{\boldsymbol{k}} \rangle$ is nontrivial. In this regime, the bath effectively decouples from the system since $M \approx 0$ and coupling to the bath is proportional to $g^2 M$. As a consequence, the system does not equilibrate and the order parameter vanishes as a power law, $M(t) \propto t^{\nu}$.

As in the damped regime, the algebraic decay in the overdamped case is also g dependent, thus differing from the $\nu = 1$ results obtained for a closed system. This is shown in Fig. 7, where we have plotted the staggered magnetization averaged over a period in log-log scale. The numerical results are fitted to a linear function $\nu_N(g)y + a$, with $y = \ln(t)$. ν is observed to vary with g: $\nu_{200}(g = 0.1) \approx 0.96$ to $\nu_{200}(g = 0.18) \approx 0.70$. Notice that the result slightly varies with system size. This is because the equilibrium staggered magnetization is very sensitive to the size of the system for these values of U. Nonetheless, it is clear that $\nu_N(g)$ is converging to a g-dependent exponent $\nu(g)$.

The transition between the overdamped and the damped regimes upon increasing g can be seen in the finite-size scaling of $M(T_N)/M(T_{\text{eq}})$ shown in Fig. 6(c). In the small-g region, $M(T_N)$ vanishes for increasing N, whereas for large g, it seems to attain a finite value. The crossing of the finite-size data is compatible with the transition arising for $0.2 < g_c < 0.24$ for the parameter values of Fig. 6(c).

V. DISCUSSION

We studied the dynamics ensuing after an interaction quench in a model consisting of a Hubbard layer coupled to an antiferromagnetic magnon bath. For vanishing system-bath coupling, within a mean-field approximation, the post-quench dynamics can be mapped to that of well-studied BCS quenches. We identify the three known asymptotic long-time regimes: persistent oscillations of the order parameter, Landau damping and overdamped. In the overdamped regime, we found that specificities of the 2D electronic density of states—a discontinuity at the band edges and a logarithmic divergence near the Fermi energy—result in a power-law decay of the order parameter rather than the exponential one reported for the BCS case that assumes a smooth density of states.

For a finite system-bath coupling, we show that the system does not always equilibrate as one would expect. Instead, three different regimes are observed at large times: an equilibrating regime, where the system attains an asymptotic equilibrium state; a damped regime, where the magnetization attains a static finite value that differs from the equilibrium one; and an overdamped regime, characterized by an asymptotically vanishing magnetization.

Each regime can be seen as a reminiscence of one of the different dynamical phases of the closed system. The persistent oscillations found in the phase-locked regime of the closed system do not survive in the presence of the bath and slowly decay to the equilibrium solution. The presence of nonequilibrium states is possible as the dissipative environment is only sensitive to time changes of the magnetization. For a static magnetization, it acts simply as a renormalization of the Hubbard interaction. Therefore, nonequilibrium phases with a static magnetization are stable. These static phases include the zero magnetized phase of the overdamped regime and a phase similar to the one obtained in the Landau-damped regime of the closed system.

We show that although the bath does not qualitatively change the dynamics in the overdamped and damped regimes, there is a difference in how the staggered magnetization approaches its asymptotic value, $M \simeq M(\infty) + O(t^{-\nu})$. For finite g, the exponent ν no longer takes the discrete values 1 or $1/2$. Instead, it seems to vary continuously in the range from $1/2$ to 1 as a function of g.

Our results are based on mean-field theory and therefore qualitatively correct only on time scales smaller than the quasiparticle lifetime τ_q. The presence of the bosonic bath introduces an additional time scale τ_g. Thus our treatment is relevant for parameter sets such that $\tau_g \ll \tau_q$. Moreover, the mean-field approximation discards quantum fluctuations of the order parameter both perpendicular and parallel to the magnetization vector. It would be interesting to investigate the effect of these fluctuations in the asymptotic long-time regime, in particular to study the survival of the nonequilibrium states found here at the mean-field level.

Nonetheless, even if all of the dynamic mean-field regimes do not survive the inclusion of quantum fluctuation, traces of these regimes should be found at time scales for which fluctuation effects can be disregarded.

ACKNOWLEDGMENTS

We gratefully acknowledge discussions with Y. E. Shchadilova and enlightening remarks on the work of S. M. Apenko. The study was funded by the RSF, Grant No.

16-42-01057. P.R. acknowledges support by FCT through the Investigador FCT Contract No. IF/00347/2014.

APPENDIX: CLOSED SYSTEM: CROSSOVER IN OVERDAMPED REGIME

Here we derive the asymptotic long-time behavior in the overdamped regime. Figure 1 (lower-right panel) shows examples of the time evolution for $h_c(t=0) \ll 8J$ and $h_c(t=0) \gg 8J$. Though the temporal behavior for $h_c(t=0) \ll 8J$ looks different from the one for $h_c(t=0) \gg 8J$, both regimes can be described by a smooth function of $h_c(t=0)$.

In the overdamped regime which arises for $U_i/U_f \gg 1$, it is therefore natural to consider an expansion around small U_f. At $U_f = 0$, one has that $\boldsymbol{B_k}(t>0) = \{0,0,\epsilon_{\boldsymbol{k}}\}$ and thus the evolution of the different momenta decouples. Starting from initial conditions (14), the evolution of the order parameter becomes

$$M(t) = \frac{1}{2}\int d\epsilon \frac{\varrho(\epsilon)}{\sqrt{1+\frac{\epsilon^2}{h_c(t=0)^2}}} e^{2i\epsilon t}, \tag{A1}$$

where $\varrho(\epsilon) = \int_k \delta(\epsilon - \epsilon_{\boldsymbol{k}})$ is the bare density of states of the electronic system.

In two spatial dimensions, $\varrho(\epsilon)$ has two distinctive features that may contribute to the asymptotic long-time behavior of $M(t)$: $\varrho(\epsilon) \propto -\ln(|\epsilon|)$ for $\epsilon \simeq 0$, and $\varrho(\epsilon)$ has sharp cutoffs at $\epsilon = \pm 4J$. The damped-oscillatory or purely damped behavior of $M(t)$ depends on the respective contribution of each of these features: the denominator in the right-hand side of Eq. (A1) defines a window of characteristic size $h_c(t=0)$ within which the integrand is non-negligible; if this window is much smaller than the bandwidth, the only singularity that contributes to the long-time behavior is the one at $\epsilon \simeq 0$ that leads to an asymptotic behavior in $1/t$. On the contrary, if the $h_c(t=0)$ is much larger than the bandwidth, there are additional oscillatory contributions coming from the nonanalyticities at the band edges that behave as $\sin(8Jt)/t$.

A more quantitative way to obtain the oscillatory-damped crossover of $M(t)$ as a function of $h_c(t=0)$ is to develop Eq. (A1) around $h_c(t=0) \simeq 4J$. Defining $\delta = h_c(t=0) - 4J$, we obtain

$$\begin{aligned} M(t) \approx & \frac{1}{8J\pi t} + \frac{\sin(8Jt)}{8J\pi\sqrt{2}t} - \frac{\delta}{2(4J)^2 t\pi (2)^{3/2}}\sin(8Jt) \\ & - \frac{3\delta^2}{4(4J)^3\pi 2^{5/2} t}\sin(8Jt) \\ & - \frac{3\delta^3}{4(4J)^4\pi 2^{7/2} t}\sin(8Jt) + O(\delta^4). \end{aligned} \tag{A2}$$

Even if the region of applicability of this expression is limited, it reproduces well the numerical results and captures the crossover behavior observed in the overdamped regime.

[1] A. Polkovnikov, K. Sengupta, A. Silva, and M. Vengalattore, Rev. Mod. Phys. **83**, 863 (2011).
[2] L. D. Landau, Zh. Eksp. Teor. Fiz. **16**, 574 (1946).
[3] L. Gor'kov and G. Eliashberg, Sov. Phys. JETP **27**, 328 (1968).
[4] A. F. Volkov and S. M. Kogan, Zh. Eksp. Teor. Fiz. **65**, 2038 (1973) [Sov. Phys. JETP **38**, 1018 (1974)].
[5] R. A. Barankov and L. S. Levitov, Phys. Rev. Lett. **96**, 230403 (2006).
[6] E. A. Yuzbashyan, O. Tsyplyatyev, and B. L. Altshuler, Phys. Rev. Lett. **96**, 097005 (2006).
[7] R. A. Barankov, L. S. Levitov, and B. Z. Spivak, Phys. Rev. Lett. **93**, 160401 (2004).
[8] A. Bulgac and S. Yoon, Phys. Rev. Lett. **102**, 085302 (2009).
[9] M. S. Foster, M. Dzero, V. Gurarie, and E. A. Yuzbashyan, Phys. Rev. B **88**, 104511 (2013).
[10] M. S. Foster, V. Gurarie, M. Dzero, and E. A. Yuzbashyan, Phys. Rev. Lett. **113**, 076403 (2014).
[11] F. Peronaci, M. Schiró, and M. Capone, Phys. Rev. Lett. **115**, 257001 (2015).
[12] D. V. Chichinadze, P. Ribeiro, Y. E. Shchadilova, and A. N. Rubtsov, Phys. Rev. B **94**, 054301 (2016).
[13] M. C. Gonzalez-Garcia, M. Maltoni, and T. Schwetz, J. High Energ. Phys. **11** (2014) 052.
[14] M. Dzero, M. Khodas, and A. Levchenko, Phys. Rev. B **91**, 214505 (2015).
[15] M. Sandri and M. Fabrizio, Phys. Rev. B **88**, 165113 (2013).
[16] N. Tsuji, M. Eckstein, and P. Werner, Phys. Rev. Lett. **110**, 136404 (2013).
[17] M. Srednicki, Phys. Rev. E **50**, 888 (1994).
[18] J. M. Deutsch, Phys. Rev. A **43**, 2046 (1991).
[19] M. Rigol, V. Dunjko, and M. Olshanii, Nature (London) **452**, 854 (2008).
[20] M. Rigol, V. Dunjko, V. Yurovsky, and M. Olshanii, Phys. Rev. Lett. **98**, 050405 (2007).
[21] E. Ilievski, J. De Nardis, B. Wouters, J.-S. Caux, F. H. L. Essler, and T. Prosen, Phys. Rev. Lett. **115**, 157201 (2015).
[22] A. Amaricci, C. Weber, M. Capone, and G. Kotliar, Phys. Rev. B **86**, 085110 (2012).
[23] G. Mazza, A. Amaricci, M. Capone, and M. Fabrizio, Phys. Rev. B **91**, 195124 (2015).
[24] E. Fradkin, *Field Theories of Condensed Matter Physics* (Cambridge University Press, Cambridge, 2013).
[25] A. Altland and B. D. Simons, *Condensed Matter Field Theory* (Cambridge University Press, Cambridge, 2010).
[26] J. Jaeckel and C. Wetterich, Phys. Rev. D **68**, 025020 (2003).
[27] P. W. Anderson, Phys. Rev. **112**, 1900 (1958).
[28] E. A. Yuzbashyan and M. Dzero, Phys. Rev. Lett. **96**, 230404 (2006).